3040 *Biochemistry* **2010,** *49,* 3040–3048
DOI: 10.1021/bi9019252

BIOCHEMISTRY
including biophysical chemistry & molecular biology
Article

Effect of Lipid Type on the Binding of Lipid Vesicles to Islet Amyloid Polypeptide Amyloid Fibrils[†]

Kenji Sasahara,*[,‡] Damien Hall,[§] and Daizo Hamada[‡]

[‡]*Division of Structural Biology, Department of Biochemistry and Molecular Biology, Graduate School of Medicine, Kobe University, 7-5-1 Kusunoki-cho, Chuo-ku, Kobe 650-0017, Japan, and* [§]*Institute of Basic Medical Science, University of Tsukuba, Lab 225-B, Building D, 1-1-1 Tennodai, Tsukuba-shi, Ibaraki-ken 305-8577, Japan*

Received November 10, 2009; Revised Manuscript Received March 8, 2010

ABSTRACT: Amyloid deposits, composed primarily of the 37-residue islet amyloid polypeptide (IAPP), are observed near pancreatic β-cells of type II diabetics, with their presence strongly correlating with a loss of β-cell mass and decreased pancreatic function. Although β-cell membranes have been implicated as the likely target of amyloidogenic IAPP toxicity, interactions between membranes and IAPP in the fibrillar state have not been well characterized. In this study, turbidity measurements were conducted to provide a detailed description of the binding reaction between IAPP fibrils and lipid vesicles made from phosphatidylcholine. The kinetic data representing the rate and extent of the fibril−vesicle binding reaction are described well by an empirical double-exponential equation. The extent of binding was found to increase with increasing amyloid fibril concentration. Modification of the vesicle composition significantly altered the observed binding reaction kinetics, with the change quantified using the parameters obtained from the double-exponential fitting analysis. When the vesicles contained a significant amount of the lipid phosphatidylglycerol, substantial sedimentation of the vesicles under gravity was detected following the initial binding reaction. To rationalize the observed kinetic binding data, we developed a mesoscopic simulation model based on a hard particle representation of the species involved. In light of the observed data and simulation predictions, the potential roles of IAPP amyloid fibrils in membrane binding are discussed.

The deposition of proteins into fibrillar amyloid is associated with the pathogenesis of various diseases, including Alzheimer's disease, Parkinson's disease, prion disease, and type II diabetes (*1*, *2*). Amyloid fibrils are commonly described as being several micrometers long, being 7−12 nm in diameter, and possessing a common structural motif consisting of cross-β-sheet structures, in which individual β-strands are perpendicular to the fibril axis (*1*, *2*). Human islet amyloid polypeptide (IAPP,[1] also known as amylin) is a 37-residue peptide (Figure 1) that is the major constituent of amyloid fibrils deposited in the pancreatic islets associated with type II diabetes mellitus (T2DM) (*3*−*9*). IAPP is synthesized in pancreatic β-cells and cosecreted with insulin in response to the same stimuli (*10*). In advanced stages of T2DM, amyloid fibrils of IAPP are extracellularly deposited near β-cells in more than 90% of patients (*4*−*6*). Substantial evidence has suggested that lipid membranes are the likely target of amyloidogenic IAPP and its fibrillation is responsible for the death of β-cells (*7*, *11*, *12*). Although causative factors for the conversion of the normally soluble IAPP to fibrillar aggregates remain unknown, chemical analyses of tissue-extracted fibrillar deposits from a number of diseases have provided evidence that constituent parts of cellular lipids can be incorporated into these deposits, suggesting a possible role for lipids in enhancing and/or facilitating aggregation of the protein into amyloid fibrils in vivo (*13*, *14*).

A number of studies about the effects of toxic IAPP on β-cell death have indicated that oligomeric or prefibrillar species exhibit higher levels of cytotoxity than mature fibrils (*15*−*20*). Although it is still not clear whether the fibrils themselves or their intermediate states cause cell death, a major hypothesis is that amyloidogenic species of IAPP, such as prefibrillar states and/or structured protofibrils, cause membrane damage through porelike action (channels) (*16*, *20*) or through detergent-like permeabilization (*11*, *21*), resulting in cytotoxicity. Cytotoxity by membrane damage associated with amyloid fibrillation has also been suggested for other amyloidogenic peptides and proteins related to Alzheimer's disease, Parkinson's disease, and prion disease (*18*−*20*).

In vitro experiments have previously established that amyloid fibrillation is significantly accelerated in the presence of lipid membranes, particularly those containing negative charges, for example, for Aβ (*22*, *23*), prion (*24*), α-synuclein (*25*, *26*), and IAPP (*27*−*30*). The fibrillation of IAPP has been demonstrated to occur upon dilution of monomeric IAPP into a physiological buffer (*31*, *32*), with this reaction strongly promoted by the presence of negatively charged lipid membranes (*27*−*30*, *33*, *34*).

[†]This research was supported by grants from the Global COE Program A08 from the Ministry of Education, Culture, Sports, Science and Technology of Japan (to D. Hamada and K. Sasahara), the Japanese Science and Technology Agency (JST) (to D. Hall), and the University of Tsukuba under the special coordinated scheme "Funds in Aid for the Promotion of Young Scientistś Independent Research" (to D. Hall).

*To whom correspondence should be addressed: Graduate School of Medicine, Kobe University, 7-5-1 Kusunoki-cho, Chuo-ku, Kobe 650-0017, Japan. E-mail: sasahara@med.kobe-u.ac.jp. Telephone: +81-78-382-5817. Fax: +81-78-382-5816.

[1]Abbreviations: IAPP, islet amyloid polypeptide; T2DM, type II diabetes mellitus; PC, phosphatidylcholine; SM, sphingomyelin; DOPS, 1,2-dioleoyl-*sn*-glycero-3-(phospho-L-serine); DMPG, 1,2-dimyristoyl-*sn*-glycero-3-[phospho-*rac*-(1-glycerol)]; CF, 5(6)-carboxyfluorescein; Aβ, amyloid β-peptide; DMSO, dimethyl sulfoxide; ThT, thioflavin T.

 Published on Web 03/08/2010 © 2010 American Chemical Society

Human IAPP KCNTATCATQRLANFLVHSSNNFGA I LSSTNVGSNTY

FIGURE 1: Amino acid sequence of human IAPP. The peptide is amidated at the C-terminus and has a disulfide bond between residues 2 and 7.

IAPP carries three positive charges at its N-terminus at neutral pH, which induces a strong attractive interaction with the negatively charged lipid headgroups (*35*−*38*). Although the molecular mechanism of such an acceleration remains elusive, it is presumed that lipid membrane-induced changes in the conformation of polypeptides could possibly promote fibril formation by enhancing nucleation (*39*). In vivo, phosphatidylserine (PS) is highly enriched on the cytoplasmic face of the lipid membrane, and studies conducted with rodent pancreatic islets indicated that PS comprises 4−14 mol % of the total phospholipid content (*40*). Furthermore, it has been suggested that alterations in lipid metabolism associated with T2DM cause changes in the lipid environment that may induce pathological effects involving amyloidogenic IAPP (*28*, *41*).

The current viewpoint is that membrane disruption and concomitant β-cell death are caused by toxic IAPP amyloid oligomers, and that relatively mature amyloid fibrils are biologically inert (*8*, *15*−*20*). On the other hand, states of association between extracellular IAPP amyloid fibrils and β-cell membranes have also been observed in which the fibrils were often oriented to β-cell membranes (*12*, *35*, *42*, *43*). However, at present, the exact identity of the membrane-bound forms of fibrillar IAPP along with a detailed characterization of the binding reaction has not been fully elucidated. In this study, we report our findings on the binding reaction between lipid vesicles and IAPP amyloid fibrils, placing our focus on understanding the mechanism of the IAPP fibril−membrane interaction. Vesicles made from the predominant plasma membrane phospholipid, phosphatidylcholine (PC), were used as our core model membrane to which other lipids, including PS, were added.

MATERIALS AND METHODS

Materials. Egg yolk L-α-phosphatidylcholine (PC) and bovine brain sphingomyelin (SM) were purchased from Sigma Chemical Co. (St. Louis, MO). 1,2-Dioleoyl-*sn*-glycero-3-(phospho-L-serine) sodium salt (COATSOME MS-8181LS: DOPS) and 1,2-dimyristoyl-*sn*-glycero-3-[phospho-*rac*-(1-glycerol)] sodium salt (COATSOME MG-4040LS: DMPG) were purchased from Wako Pure Chemical Industries Ltd. (Osaka, Japan). Human IAPP and amyloid β-peptides [Aβ(1−42) and Aβ(25−35)] were purchased from Peptide Institute, Inc. (Osaka, Japan), their purity being >95% according to the elution pattern of high-performance liquid chromatography. The lipids and peptides were used without further purification. 5(6)-Carboxyfluorescein (CF) was obtained from Merck (Darmstadt, Germany). NaCl and sodium phosphates of analytical grade were obtained from Nakalai Tesque Inc. (Kyoto, Japan). Thioflavin T (ThT), dimethyl sulfoxide (DMSO), and chloroform were obtained from Wako Pure Chemical Industries Ltd. Pure (deionized and distilled) water was used for the preparation of all the solutions. Three stock solutions of 0.25 M sodium phosphate buffer (pH 7.2), a 1 M NaCl solution, and a 100 μM ThT solution were prepared using pure water and passed through a filter (pore size, 0.2 μm).

Formation of IAPP Amyloid Fibrils. IAPP was dissolved in dimethyl sulfoxide (DMSO) at 4 mg/mL and diluted with pure water to create a 0.4 mg/mL stock solution. Amyloid fibrils of IAPP were formed spontaneously when small volumes of an IAPP stock were added to polymerizing buffer [50 mM sodium phosphate and 100 mM NaCl (pH 7.2)] at 37 °C and incubated overnight (final concentration of IAPP of 78 μg/mL).

Preparation of Lipid Vesicles. Five types of lipid vesicles were prepared as follows. PC and PC/SM and PC/DOPS mixtures were dissolved in chloroform, while DMPG and PC/DMPG mixtures were dissolved in a chloroform/methanol mixture at a 2/1 (v/v) ratio. The mixing ratio of two lipids was 1/1 (w/w). After evaporation of organic solvents under atmospheric pressure, dried films were placed in a vacuum desiccator for 4 h to completely evaporate any residual solvent. Pure water was added to the dried films to yield a lipid concentration of 5−10 mg/mL, followed by mild agitation to ensure complete mixing and hydration of the lipids. The lipid suspensions in pure water were extruded 21 times through a polycarbonate filter of 100 (or 50) nm pore sizes by a mini-extruder (Avanti Polar Lipids Inc., Birmingham, AL). The sizes of the vesicles were confirmed according to dynamic light scattering measurements (DLS-6500, Otsuka Electronics Co., Ltd.).

Turbidity Measurements. Turbidity measurements were conducted in investigating the kinetics of the binding reaction between amyloid fibrils and lipid vesicles at pH 7.2 and 25 °C. The vesicles in pure water were diluted to the desired concentrations with the stock solutions of phosphate and NaCl at pH 7.2 (final buffer of 50 mM phosphate and 100 mM NaCl) before being mixed with amyloid fibrils. The fibril solution including the same buffer was manually added to the vesicle solution in a test tube, and the sample solution was agitated for 3 s using a benchtop vortex mixer. Immediately after the mixed sample solution had been placed into a quartz cuvette (path length of 10 mm), time-dependent changes in solution turbidity were measured for 1 h [recorded as the apparent absorption at 600 nm (Abs_{600})] using a JASCO V-550 spectrophotometer. The time interval from the initiation of mixing to the first measurement was 40 s (i.e., dead time of the kinetic measurement). The turbidity of the samples 24 h after mixing was measured following agitation for 3 s using the same vortex mixer. The temperature of the sample was maintained at 25 ± 0.1 °C by circulating water from a thermostat bath.

Data Analysis. The time-dependent appearance of solution turbidity following the mixing of amyloid fibrils and vesicles was fitted to a single exponential (eq 1) or double exponential (eq 2).

$$A(t) = A(\infty) + \Delta A \exp(-k_{app} t) \quad (1)$$

$$A(t) = A(\infty) + \Delta A_1 \exp(-k_{1,app} t) + \Delta A_2 \exp(-k_{2,app} t) \quad (2)$$

where $A(t)$ and $A(\infty)$ are the observed values of the turbidity values at time t and infinite time, respectively, and ΔA and k_{app} refer to the amplitude and the apparent rate constant of the observed phases, respectively.

ThT Fluorescence Measurements. Aliquots of a 20 μg/mL protein solution were mixed with 100 μM thioflavin T (ThT), resulting in a solution containing 19 μg/mL protein and 5 μM ThT. The intensity of the fluorescence from ThT in the mixed solution was monitored with a JASCO FP-6500 spectrofluorometer using a quartz cell with a light path of 5 mm. ThT fluorescence was excited at 445 nm (5 nm slit width), and the emission was recorded at 485 nm (5 nm slit width). The temperature of the sample solutions was maintained at 25 ± 0.1 °C by circulating water from a thermostat.

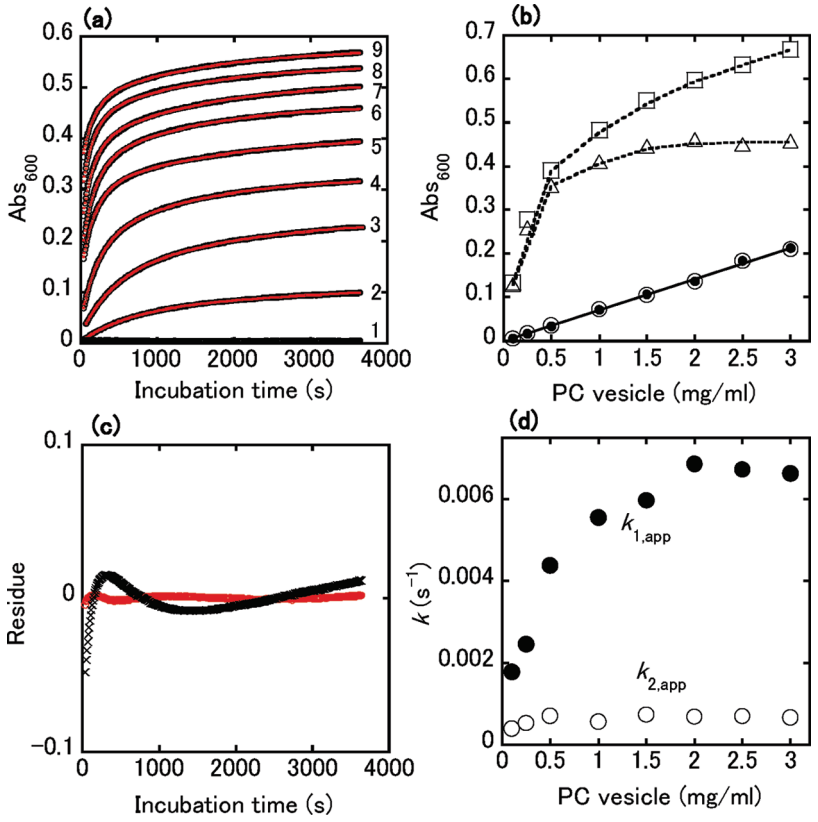

FIGURE 2: Dependence of PC vesicle concentration on the binding reaction with IAPP fibrils at 25 °C and pH 7.2. (a) Time-dependent changes in solution turbidity of IAPP fibrils (25 μg/mL) and PC vesicles at various concentrations (0−3.0 mg/mL): vesicle concentrations of 0 (1), 0.1 (2), 0.25 (3), 0.5 (4), 1.0 (5), 1.5 (6), 2.0 (7), 2.5 (8), and 3.0 mg/mL (9) (from bottom to top). Black and red symbols represent the experimental data and the best fit of each data set to eq 2, respectively. (b) Apparent absorbance of the vesicle solutions and mixed fibril/vesicle solutions. The apparent absorbance of the PC vesicle solutions without IAPP fibrils was measured twice within 24 h of dilution with the buffer: just after the dilution (○) and after 24 h (●). Apparent absorbances of the fibril/vesicle solutions after being mixed for 24 h in panel a are indicated before (□) and after (△) subtraction of the turbidity of the respective PC vesicle components. (c) Residues between the observed and fitted values. The observed values of sample 5 in panel a were fitted to eqs 1 and 2, and the residues from the fittings to eq 1 (black symbols) and eq 2 (red symbols) were estimated. (d) Dependence of apparent rate constants, $k_{1,app}$ and $k_{2,app}$, on the PC vesicle concentration. Two k_{app} values were evaluated by fitting the data in panel a to eq 2, in which $k_{1,app}$ and $k_{2,app}$ were assigned to the fast and slow phase, respectively.

RESULTS

Binding Reaction between IAPP Fibrils and PC Vesicles. Binding reactions between IAPP fibrils and PC vesicles were monitored at 25 °C by the time-dependent appearance of solution turbidity, measured as the apparent absorbance at 600 nm (Abs_{600}). Solutions of amyloid fibrils and lipid vesicles were made up in identical buffers at pH 7.2 (50 mM phosphate and 100 mM NaCl). Images of IAPP fibrils prepared in the polymerizing buffer were acquired by electron microscopy and revealed morphology typical of amyloid fibrils (Figure S1 of the Supporting Information). Vesicles prepared by extrusion through a filter with a pore size of 100 nm were used except in the cases specified. Binding reactions were induced by addition of a solution of IAPP fibrils (final concentration of 25 μg/mL) to PC vesicle solutions at various concentrations, followed by continuous absorbance measurement for 1 h. As one can see in Figure 2a, the time-dependent turbidity of the mixed solutions significantly increased with increasing concentrations of PC vesicles (lines 2−9), compared to that of the fibril solution without the vesicles (line 1).

We confirmed the stability of PC vesicles by monitoring the change in solution turbidity over a 24 h period (Figure 2b). No detectable recorded change in Abs_{600} confirmed the stability of the vesicles over this time region (filled and empty circles in Figure 2b), with the size of the vesicles being considerably smaller than the transition size determined by Pozharski et al. (*44*) at which turbidity becomes independent of the increasing size and dependent on the lipid weight concentration only. Abs_{600} values were taken from the samples in Figure 2a, 24 h after initiation of mixing, and plotted versus the vesicle concentration (squares in Figure 2b). These corresponding values corrected for contribution of starting vesicle concentration are also shown (triangles in Figure 2b). The latter values indicate asymptotic behavior typical of a saturable process. Taken together, the experimental demonstration of the stability of the vesicle turbidity and the experimental observation of a stable end point for the vesicle−amyloid interaction imply that the time-dependent traces of turbidity recorded for 1 h in Figure 2a represent a nondestructive binding reaction between IAPP fibrils and PC vesicles.

Additionally, the stability of the vesicles associated with IAPP fibrils was confirmed via examination of the leakage of PC vesicles loaded with carboxyfluorescein (CF). The CF release kinetics was investigated after the vesicles were mixed with IAPP fibrils (Figure S2 of the Supporting Information). Dye release was not observed for the vesicles incubated with IAPP fibrils over the time period of 48 h as well as the fibril-free vesicle solution. In contrast, when the PC vesicles were incubated with a detergent [i.e., sodium dodecyl sulfate (SDS)], the fluorescence intensity increased considerably as a result of the release of the encapsulated dye to bulk solvent, indicating that the disruption of membranes had occurred.

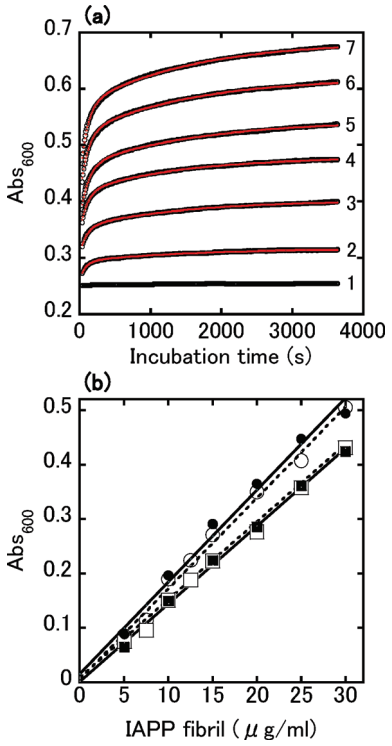

FIGURE 3: Dependence of IAPP fibril concentration on the binding reaction with PC vesicles at 25 °C and pH 7.2. (a) Time-dependent changes in the apparent solution absorbance of IAPP fibrils at various concentrations (0−30 μg/mL) and PC vesicles (3.0 mg/mL): fibril concentrations of 0 (1), 5 (2), 10 (3), 15 (4), 20 (5), 25 (6), and 30 μg/mL (7) (from bottom to top). Black and red symbols represent the experimental data and the fitted values, respectively. (b) Apparent solution absorbance after mixing for 1 and 24 h. The apparent solution absorbance of the samples in panel a was plotted vs the concentration of IAPP fibrils after subtraction of that of the respective PC vesicle components: after 1 h (■) and 24 h (●). Similarly, the apparent solution absorbance was plotted for the samples including the PC vesicles extruded through a 50 nm pore: after 1 h (□) and 24 h (○). Solid and dotted lines were linearly best fitted to the filled and empty symbols, respectively.

The turbidity data presented in Figure 2a were subjected to nonlinear least-squares regression analysis in terms of a single exponential (eq 1) or sum of exponential processes (eq 2). As can be noted by the residual plot (Figure 2c), the data were fit by a sum of two exponential processes (red lines in Figure 2a). The two apparent rate constants obtained by the best fit to eq 2 corresponded to a fast phase ($k_{1,app}$) and a slow phase ($k_{2,app}$). When plotted against vesicle concentration (Figure 2d), $k_{1,app}$ roughly increased with increasing vesicle concentration, whereas $k_{2,app}$ was largely independent of vesicle concentration.

To further examine the binding reaction between fibrils and vesicles, a reverse assay format was adopted. In this approach, IAPP fibril solutions at various concentrations were added to a solution of PC vesicles at 3.0 mg/mL and the apparent absorbance at 600 nm (Abs_{600}) was recorded (black symbols in Figure 3a) (best fit agreement to eq 2 colored red). Vesicle-corrected Abs_{600} values of the sample solutions, measured 1 h (■) and 24 h (●) after mixing, were plotted versus the concentration of the fibrils in the samples (Figure 3b). These plots indicated a linear dependence of solution turbidity on fibril concentration. To further test this apparent linear dependence, we repeated the same experiment using PC vesicles extruded through a different pore size of 50 nm and made the same plot for the resultant Abs_{600} values. This second experiment also showed a linear dependence of Abs_{600} on the fibril concentration (empty symbols in Figure 3b). Figure 3b suggests that the extent of binding of PC vesicles to the surface of amyloid fibrils is enhanced in direct proportion to the concentration of IAPP fibrils when they exist under conditions of excess vesicle concentration.

Binding Reaction between PC Vesicles and Aβ Amyloid Fibrils. It is widely accepted that the fibrillization of the Aβ peptide (composed of 40−42 amino acids) plays an important role in the pathogenesis of Alzheimer's disease (*23*). To examine the binding reaction of other amyloid fibrils with PC vesicles, the time dependence of Abs_{600} was also recorded for amyloid fibrils formed from Aβ(1−42) and Aβ(25−35) (Figure S3 of the Supporting Information). For the sake of comparison, the same measurement was conducted for IAPP fibrils under identical conditions (Figure S3). The time-dependent appearance of solution turbidity was observed for the two Aβ amyloid fibrils; however, its magnitude was less than that for IAPP fibrils, implying a weaker binding affinity of PC vesicles for Aβ amyloid fibrils.

Effect of Fibrillation State of IAPP on the Binding Reaction with PC Vesicles. The effect of the fibrillation state of IAPP on the binding reaction with PC vesicles was examined using a modified turbidity assay. First, 0.4 mg/mL solutions of IAPP including water and DMSO (see Materials and Methods) were mixed with PC vesicles dispersed in water and the polymerizing buffer (or pure water), resulting in solutions containing 20 μg/mL IAPP and 2.0 mg/mL PC vesicles and buffer components at several concentrations (0−15 mM). Turbidity measurements were conducted for respective solutions just after mixing. Incubation of the buffer-free solution showed no noticeable increase in Abs_{600} (line 1 in Figure 4a). As indicated by the increase in Abs_{600}, acceleration of the vesicle−amyloid binding interaction was promoted by increased amounts of buffer components (Figure 4a). A diagnostic amyloid-sensitive dye, thioflavin T (ThT) (*45*), was employed to determine whether the acceleration of turbidity development corresponded to an increase in the level of amyloid fibril formation (Figure 4b). A ThT fluorescence assay was conducted for the samples shown in Figure 4a immediately after results had been recorded. The results show that ThT fluorescence was enhanced by increasing amounts of polymerizing buffer components present at initiation (Figure 4b), indicating that the acceleration of the binding reaction between vesicle and amyloid observed in Figure 4a is due to an increasing extent of buffer-induced amyloid fibril formation.

Effects of Lipid Composition on the Binding Reaction. Lipid composition is considered to be one of the primary factors determining the extent to which membranes facilitate the fibrillar aggregation of peptides or proteins (*23*−*30*). To gain information about the effects of vesicle composition on the binding reaction with IAPP fibrils, PC vesicles containing zwitterionic sphingomyelin (SM) [i.e., (PC+SM) vesicles; mixing ratio of 1/1 (w/w)] were prepared for the turbidity assay. Sphingomyelin is a major sphingolipid of mammalian cells and an important component of the plasma membranes of eukaryotic cells (*46*). A solution of IAPP fibrils (final concentration of 25 μg/mL) was added to (PC+SM) vesicle solutions, and the turbidity was recorded as shown in Figure 5a. The binding reaction was detected through the time-dependent traces of Abs_{600}, which were fitted to eq 2 (red marks in Figure 5a). Compared to the binding behavior of PC vesicles, slower increases in Abs_{600} were observed during the initial stage (~1000 s) of the binding reaction. This behavior may

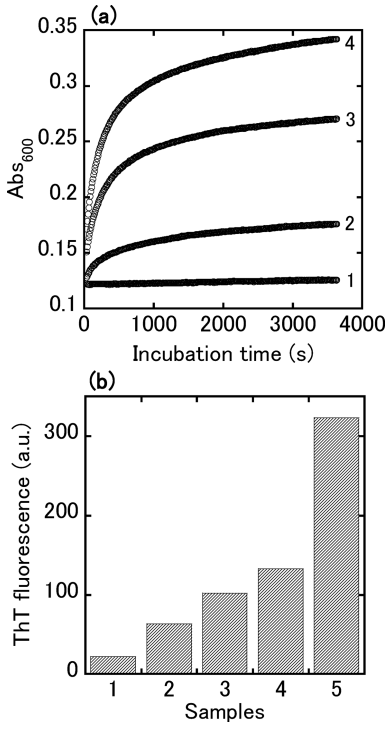

FIGURE 4: Binding reaction of PC vesicles with buffer-induced IAPP fibrils at 25 °C. (a) Time-dependent appearance of the apparent solution absorbance of buffer-induced IAPP fibrils and PC vesicles. Fibrillation was induced by mixing the polymerizing buffer at the different final concentrations with the aqueous solution containing dissolved IAPP and dispersed PC vesicles: buffer-free (1), 0.5 mM phosphate and 1 mM NaCl buffer (2), 1.7 mM phosphate and 3.4 mM NaCl buffer (3), and 5 mM phosphate and 10 mM NaCl buffer (4). The concentrations of IAPP and PC vesicles were 20 μg/mL and 2.0 mg/mL, respectively. (b) Changes in ThT fluorescence intensity. The ThT fluorescence assay was conducted for the samples 1−4 in panel a which were taken out immediately after the completion of the apparent absorbance measurements. Samples 1−4 correspond to those used in panel a. Sample 5 consisted of IAPP fibrils formed in polymerizing buffer at 37 °C overnight.

be attributable to intrinsic structural differences between SM and PC at the interfacial region due to traits relating to SM's reduced mobility and tendency to cluster within the vesicle and the different hydrophobic natures of the two lipids.

It has been reported previously that a net negative charge of the membrane significantly accelerates the fibrillation of cationic IAPP compared to zwitterionic membranes (*27*−*30*). To impart negative charge to PC vesicles, 50% (w/w) dioleoylphosphatidylserine (DOPS) was included in PC vesicles as the anionic phospholipid component [i.e., (PC+DOPS) vesicles]. Similar to the preceding case, a solution of IAPP fibrils (final concentration of 25 μg/mL) was added to these vesicle solutions at several different concentrations and the binding reaction monitored (Figure 5b). The results indicate greater increases in Abs_{600} development during the initial time stage of 0−1000 s than those measured for PC vesicles not containing DOPS.

The stability of the two vesicle types used for panels a and b of Figure 5 was checked according to the method used in Figure 2b. For the (PC+DOPS) vesicles shown in Figure 5b, the observed Abs_{600} values after incubation for 24 h were plotted versus the vesicle concentration before and after subtraction of the contribution of turbidity from the respective vesicle components (Figure 5c). The $k_{1,app}$ and $k_{2,app}$ values obtained from nonlinear least-squares regression analysis of the data shown in panels a and b of Figure 5 using eq 2 were plotted against the respective vesicle concentrations (along with the PC data from Figure 2d) (Figure 5d). The vesicle concentration dependence of the $k_{1,app}$ values corresponding to the rapid phase of the binding reaction varied significantly with the alteration in lipid composition, particularly for negatively charged (PC+DOPS) vesicles, whereas that of $k_{2,app}$ values did not show a large variation for the three types of vesicles studied.

Sedimentation of Vesicles following Binding by IAPP Fibrils. Phosphatidylglycerol is the most abundant anionic phospholipid present in the prokaryotic cell membrane and has been extensively studied as a model for the negatively charged biomembrane (*47*). Dimyristoylphosphatidylglycerol (DMPG) contains a short hydrophobic alkyl chain, and its gel−liquid crystalline phase transition occurs at ∼24 °C (*47*). To investigate the binding behavior of vesicles containing DMPG by IAPP fibrils, DMPG was included in PC vesicles [i.e., (PC+DMPG) vesicles; mixing ratio of 1/1 (w/w)]. Following addition and mixing of IAPP fibrils (final concentration of 25 μg/mL) with the (PC+DMPG) vesicle solutions, a rapid increase in Abs_{600} was observed (Figure 6a). The stability of vesicles was verified using the same method as in Figures 2b and 5c (Figure 6b). For the samples in Figure 6a, the Abs_{600} values after 1 h (△) and 24 h (□) were plotted as a function of vesicle concentration, showing that the Abs_{600} values after 24 h were generally smaller than those after 1 h over a large vesicle concentration range (Figure 6b). This result strongly suggests that the amyloid vesicle complexes sedimented under gravity to a significant extent.

To examine more closely the amyloid−vesicle complex sedimentation process, vesicles consisting solely of DMPG were prepared and mixed with the solution of IAPP fibrils at several concentrations (Figure 6c). Compared to the small Abs_{600} values recorded for the DMPG vesicle solutions without fibrils, the mixed samples revealed a remarkable increase in Abs_{600} during the time regime from 0 to 3000 s, probably due to high-order association between vesicle-coated amyloid fibrils, followed by a decrease in Abs_{600} over the time regime from 3000 to 7000 s (Figure 6c). The observed maximum in Abs_{600} increased with an increase in fibril concentration (traces 1−5 in Figure 6c).

Very similar behavior was also observed for the mixed solutions of DMPG vesicles and amyloid fibrils of Aβ(1−42), although the enhancement of turbidity was less pronounced and a longer incubation period was needed to detect the sedimentation of the vesicle−amyloid complex from the kinetic trace of the apparent absorbance (Figure 6d). To test the hypothesis that the vesicle−amyloid complexes were sedimenting under gravity due to their very large sizes, images of the sedimented fractions were taken using an optical microscope upon completion of experiments shown in panels c and d of Figure 6. These observations indicated the presence of enormous aggregates of the vesicles and amyloids (see Figure S4 of the Supporting Information for the sample in Figure 6c). Consequently, the results in panels c and d of Figure 6, together with the binding data obtained in this study, show that amyloid fibrils of IAPP and Aβ have an ability to form both low-order and high-order association complexes with lipid vesicles.

DISCUSSION

Recent studies have shown that lipid membranes can significantly increase the rate of IAPP fibrillation, with the degree of rate enhancement being strongly dependent upon the lipid

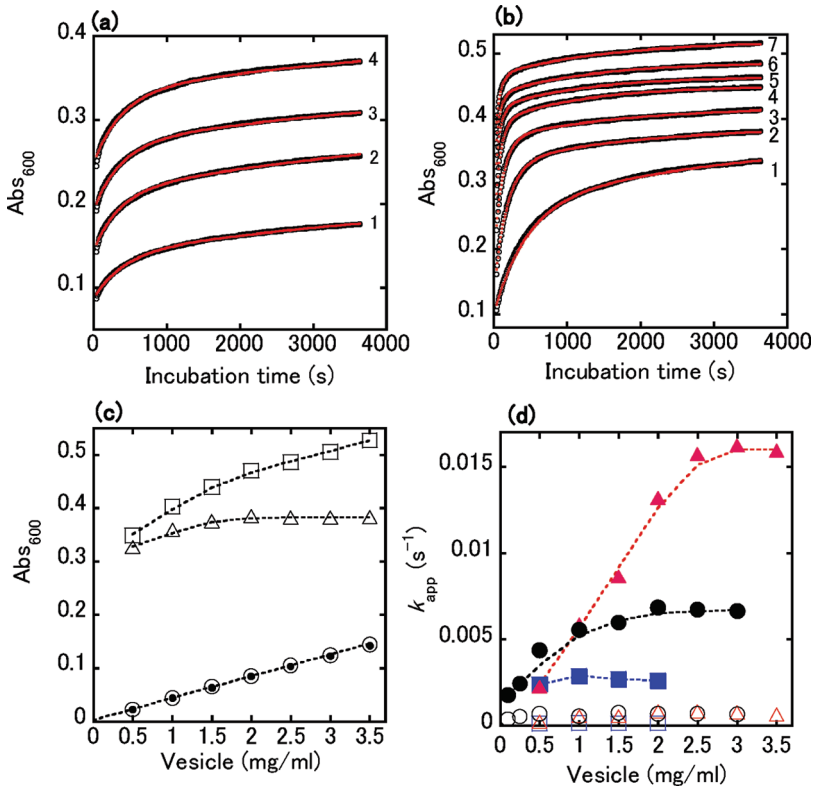

FIGURE 5: Binding reaction between (PC+SM) or (PC+DOPS) vesicles and IAPP fibrils at 25 °C and pH 7.2. (a and b) Time-dependent appearance of the apparent solution absorbance of IAPP fibrils (25 μg/mL) and (PC+SM) (a) and (PC+DOPS) (b) vesicles at various concentrations: vesicle concentrations of (a) 0.5 (1), 1.0 (2), 1.5 (3), and 2.0 mg/mL (4) and (b) 0.5 (1), 1.0 (2), 1.5 (3), 2.0 (4), 2.5 (5), 3.0 (6), and 3.5 mg/mL (7). Black and red marks represent the experimental data and the fitted values, respectively. (c) Apparent solution absorbance of the samples in panel b. The apparent absorbance of vesicle solutions without the fibrils was measured twice in a similar way in Figure 2b: just after the dilution with the buffer (○) and after 24 h (●). The apparent absorbance of the sample solutions after they had been mixed for 24 h was indicated before (□) and after (△) subtraction of that of the attendant vesicle components. (d) Dependence of $k_{1,app}$ and $k_{2,app}$ on vesicle concentration. The k_{app} values were obtained by fitting the data set in panels a and b to eq 2. Filled squares ($k_{1,app}$) and empty squares ($k_{2,app}$) were from panel a, and filled triangles ($k_{1,app}$) and empty triangles ($k_{2,app}$) were from panel b. Filled and open circles were the same as in Figure 2d.

concentration and charge density of the membranes (*27*−*30*). A simple interpretation of such a finding is that lipid membranes preferentially stabilize amyloid in the aggregated or fibrillar state. In this study, measurements of the time dependence of solution turbidity provided a detailed description of the binding reaction between IAPP fibrils and lipid vesicles. As shown in Figure 3b, the extent of binding between IAPP fibrils and PC vesicles was significantly enhanced by increasing the amount of IAPP fibrils under conditions of vesicle excess, suggesting a binding mode that involved adsorption of a PC vesicle to the surface of the IAPP fibril. Furthermore, the incubation of IAPP fibrils with PC vesicles containing anionic DOPS resulted in a more rapid increase in Abs_{600} over the time range of 0−1000 s compared to that observed with PC vesicles (Figure 5b), indicating a strong electrostatic component to the binding process. The turbidities generated by solutions of vesicles and amyloid/vesicle mixtures were shown to be stable for at least 24 h, consistent with the results from the vesicle leakage assay (Figure S2 of the Supporting Information). Taken together, all of these results suggest that the membrane environments may help drive the fibrillation of soluble IAPP by lowering the overall free energy of the protein in the fibrillar state. Our experimental observation of the stable membrane-bound forms of IAPP fibrils is in line with the results reported by Kinnunen et al. (*48*), which demonstrated that prolonged incubation of IAPP fibrils with anionic lipids causes the wrapping of the cationic IAPP fibrils by the lipid membrane.

As shown in this study, the time-dependent traces of turbidity were described well by a sum of two exponential processes, yielding two rate constants ($k_{1,app}$ and $k_{2,app}$). Currently, we do not have any experimental data to explain why the turbidity traces are described well by a double exponential. However, we tried to provide a possible rationalization using a mesoscopic simulation model based on treatment of the vesicle amyloid interaction as an interaction between cylindrical and spherical geometric objects (see the kinetic model of vesicle binding to amyloid fibrils in the Supporting Information). The model calculates the probability function regulating the binding of vesicles to amyloid fibrils using a hard particle overlap criterion in conjunction with a Monte Carlo sampling process (Figure S5 of the Supporting Information). In this model, the probability function value decreases with increasing numbers of bound vesicles, producing in the simulated kinetic binding curves both a rapid and a slow phase like the ones characterized by $k_{1,app}$ and $k_{2,app}$ in this work. The introduction of this probability function into a rate equation describing the binding reaction could reproduce the turbidity data detected experimentally on some level (Figure S6 of the Supporting Information).

It is noteworthy that IAPP fibril solutions contain a small amount of DMSO (≤0.63%, v/v). However, as shown in Figures 2b and 5c, Abs_{600} values for the mixed solutions of IAPP fibrils and vesicles exhibited a tendency to be saturated as the vesicle content increased. Furthermore, the solution turbidity increased linearly against the amount of fibrils added to the

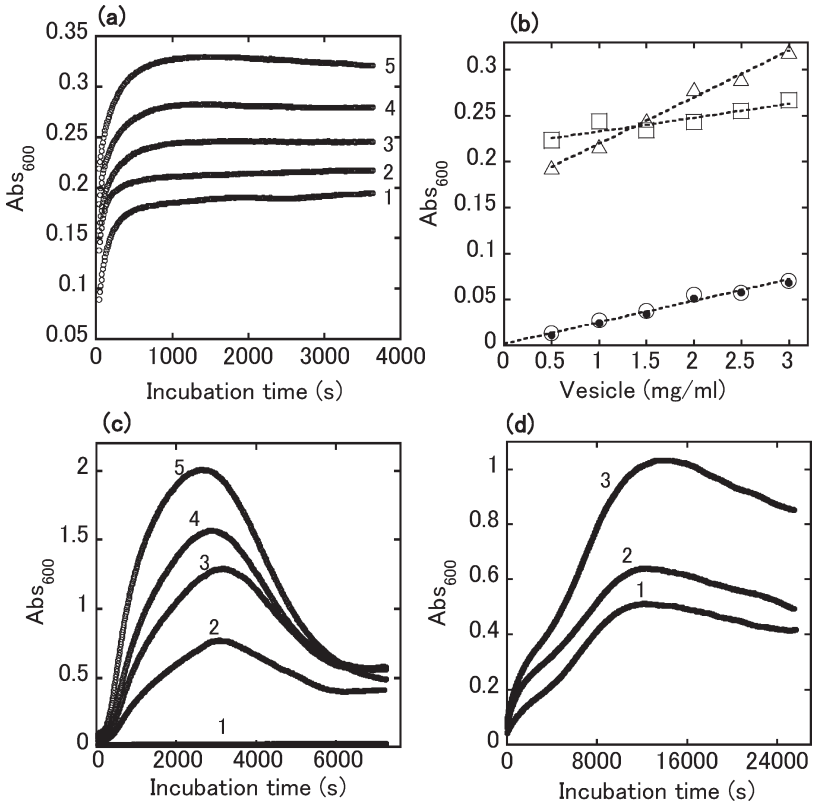

FIGURE 6: Vesicle deposition by IAPP fibrils at 25 °C and pH 7.2. (a) Time-dependent appearance of the apparent solution absorbance of IAPP fibrils (25 μg/mL) and (PC+DMPG) vesicles at various concentrations: vesicle concentrations of 0.5 (1), 1.0 (2), 1.5 (3), 2.0 (4), and 3.0 mg/mL (5) (from bottom to top). (b) Apparent absorbance of the vesicle solutions and the mixed fibril/vesicle solutions. The apparent absorbance of vesicle solutions without the fibrils was measured twice in a similar fashion in Figure 2b: just after the dilution with the buffer (○) and after 24 h (●). Apparent absorbances of the fibril/vesicle solutions after they had been mixed for 1 and 24 h in panel a are indicated: after 1 h (△) and after 24 h (□). (c and d) Time-dependent variation in the apparent solution absorbance of DMPG vesicles (2.0 mg/mL) and IAPP fibrils (c) or Aβ(1−42) fibrils (d) at several concentrations: (c) IAPP fibril concentrations of 5 (2), 10 (3), 15 (4), and 20 μg/mL (5) and (d) Aβ fibril concentrations of 10 (1), 15 (2), and 20 μg/mL (3). Trace 1 in panel c represents the apparent absorbance trace of a DMPG vesicle solution without the fibrils.

vesicle solutions (Figure 3b). These results support the notion that such a low concentration of DMSO has little effect on lipid membrane structure, consistent with the previously reported results (*28*, *49*, *50*).

In this study, PC vesicles were found to specifically bind to IAPP amyloid fibrils. Additionally, the results in panels a and b of Figure 4 demonstrate that PC vesicles can bind to just initiated fibrillar species as well as mature fibrils (as demonstrated by the increase in solution turbidity). With regard to the binding reaction with PC vesicles, amyloid fibrils of Aβ(1−42) and Aβ(25−35) exhibited behaviors similar to that shown by IAPP fibrils (Figure S3 of the Supporting Information), although the extents of binding were of lower magnitude. This result may suggest that the binding of PC vesicles to amyloid fibrils is a general behavior, the extent of which depends on the hydrophobicity and charge of the fibril surface or its morphology. As shown in panels a and b of Figure 6, when PC vesicles included anionic DMPG, sedimentation of the vesicles was detected from the turbidity behavior after they were mixed with IAPP fibrils. Substantial sedimentation of the vesicles was verified for the interaction of the DMPG vesicle with IAPP fibrils as well as with Aβ(1−42) fibrils (Figure 6c,d).

Disruption of the lipid membranes and formation of porelike channels in the membranes by oligomeric or fibrillar species are believed to make up a central mechanism of cytotoxicity of amyloid aggregates in T2DM, Alzheimer's disease, Parkinson's disease, and other amyloid-related diseases (*18*−*20*, *51*, *52*). With an enhanced awareness of the potential cytotoxity of amyloid oligomers in general, special attention has been placed on understanding the mechanism of lipid membrane disruption exerted by IAPP amyloid oligomers. It has been proposed that transient α-helical conformations of membrane-bound IAPP are precursors to the fibrillation (*27*, *34*, *53*). More recently, Engel et al. have shown that growth of IAPP fibrils is responsible for membrane disruption (*54*). Other recent research has indicated that membrane disruption of toxic IAPP can occur in a manner independent of its fibrillation (*55*). Solid-state NMR results suggest that membrane fragmentation is induced by aggregation of amyloidogenic fragments of IAPP on a lipid bilayer surface, leading to peptide/lipid vesicles (*56*). Clarifying the causative factors in membrane disruption by amyloidogenic IAPP is an active area of investigation. In this study, we placed our focus on understanding the membrane affinity of IAPP amyloid fibrils and fibril-mediated aggregation of lipid vesicles. The results of our study indicate that amyloid fibrils of IAPP and Aβ(1−42), which are proteinaceous nanoscale linear aggregates, have a latent ability to perturb lipid vesicles by binding to them, with this binding ability being both peptide- and lipid-specific.

ACKNOWLEDGMENT

We acknowledge Prof. D. M. Standley and Dr. K. Morigaki for providing useful comments on an early draft of the manuscript.

SUPPORTING INFORMATION AVAILABLE

Additional materials and methods, TEM image of IAPP fibrils (Figure S1), effect of IAPP fibrils on PC vesicle permeability (Figure S2), binding of PC vesicles to Aβ amyloid fibrils (Figure S3), image of the IAPP fibril−DMPG vesicle complex (Figure S4), kinetic model of vesicle binding to amyloid fibrils, mode of interaction in the model (Figure S5), and model with no higher-order intermolecular associations (Figure S6). This material is available free of charge via the Internet at http://pubs.acs.org.

REFERENCES

1. Selkoe, D. J. (2003) Folding proteins in fatal ways. *Nature 426*, 900–904.
2. Chiti, F., and Dobson, C. M. (2006) Protein misfolding, functional amyloid, and human disease. *Annu. Rev. Biochem. 75*, 333–366.
3. Lorenzo, A., Razzabonl, B., Weir, G. C., and Yankner, B. A. (1994) Pancreatic islet cell toxicity of amylin associated with type-2 diabetes mellitus. *Nature 368*, 756–760.
4. Kahn, S. E., Andrikopoulos, S., and Verchere, C. B. (1999) Islet amyloid: A long-recognized but underappreciated pathological feature of type 2 diabetes. *Diabetes 48*, 241–253.
5. Clark, A., and Nilsson, M. R. (2004) Islet amyloid: A complication of islet dysfunction or an aetiological factor in type 2 diabetes? *Diabetologia 47*, 157–169.
6. Höppener, J. W. M., and Lips, C. J. M. (2006) Role of islet amyloid in type 2 diabetes mellitus. *Int. J. Biochem. Cell Biol. 38*, 726–736.
7. Khemtémourian, L., Killian, J. A., Höppener, J. W. M., and Engel, M. F. M. (2008) Recent insights in islet amyloid polypeptide-induced membrane disruption and its role in β-cell death in type 2 diabetes mellitus. *Exp. Diabetes Res. 2008*, 1–9.
8. Haataja, L., Gurlo, T., Huang, C. J., and Butler, P. C. (2008) Islet amyloid in type 2 diabetes, and the toxic oligomer hypothesis. *Endocr. Rev. 29*, 303–316.
9. Hull, R. L., Westermark, G. T., Westermark, P., and Kahn, S. E. (2004) Islet amyloid: A critical entity in the pathogenesis of type 2 diabetes. *J. Clin. Endocrinol. Metab. 89*, 3629–3643.
10. Kahn, S. E., D'Alessio, D. A., Schwartz, M. W., Fujimoto, W. Y., Ensinck, J. W., Taborsky, G. J., Jr., and Porte, D., Jr. (1990) Evidence of cosecretion of islet amyloid polypeptide and insulin by β-cells. *Diabetes 39*, 634–638.
11. Jayasinghe, S. A., and Langen, R. (2007) Membrane interaction of islet amyloid polypeptide. *Biochim. Biophys. Acta 1768*, 2002–2009.
12. Engel, M. F. M. (2009) Membrane permeabilization by islet amyloid polypeptide. *Chem. Phys. Lipids 160*, 1–10.
13. Gellermann, G. P., Appel, T. R., Tannert, A., Radestock, A., Hortschansky, P., Schroeckh, V., Leisner, C., Lütkepohl, T., Shtrasburg, S., Röcken, C., Pras, M., Linke, R. P., Diekmann, S., and Fändrich, M. (2005) Raft lipids as common components of human extracellular amyloid fibrils. *Proc. Natl. Acad. Sci. U.S.A. 102*, 6297–6302.
14. Radovan, D., Opitz, N., and Winter, R. (2009) Fluorescence microscopy studies on islet amyloid polypeptide fibrillation at heterogeneous and cellular membrane interfaces and its inhibition by resveratrol. *FEBS Lett. 583*, 1439–1445.
15. Janson, J., Ashley, R. H., Harrison, D., McIntyre, S., and Butler, P. C. (1999) The mechanism of islet amyloid polypeptide toxicity is membrane disruption by intermediate-sized toxic amyloid particles. *Diabetes 48*, 491–498.
16. Anguiano, M., Nowak, R. J., and Lansbury, P. T., Jr. (2002) Protofibrillar islet amyloid polypeptide permeabilizes synthetic vesicles by a pore-like mechanism that may be relevant to type II diabetes. *Biochemistry 41*, 11338–11343.
17. Porat, Y., Kolusheva, S., Jelinek, R., and Gazit, E. (2003) The human islet amyloid polypeptide forms transient membrane-active prefibrillar assemblies. *Biochemistry 42*, 10971–10977.
18. Kayed, R., Sokolov, Y., Edmonds, B., McIntire, T. M., Milton, S. C., Hall, J. E., and Glabe, C. G. (2004) Permeabilization of lipid bilayers is a common conformation-dependent activity of soluble amyloid oligomers in protein misfolding diseases. *J. Biol. Chem. 279*, 46363–46366.
19. Demuro, A., Mina, E., Kayed, R., Milton, S. C., Parker, I., and Glabe, C. G. (2005) Calcium dysregulation and membrane disruption as a ubiquitous neurotoxic mechanism of soluble amyloid oligomers. *J. Biol. Chem. 280*, 17294–17300.
20. Quist, A., Doudevski, I., Lin, H., Azimova, R., Ng, D., Frangione, B., Kagan, B., Ghiso, J., and Lal, R. (2005) Amyloid ion channels: A common structural link for protein-misfolding disease. *Proc. Natl. Acad. Sci. U.S.A. 102*, 10427–10432.
21. Green, J. D., Kreplak, L., Goldsbury, C., Blatter, X. L., Stolz, M., Cooper, G. S., Seelig, A., Kistler, J., and Aebi, U. (2004) Atomic force microscopy reveals defects within mica supported lipid bilayers induced by the amyloidogenic human amylin peptide. *J. Mol. Biol. 342*, 877–887.
22. McLaurin, J., Franklin, T., Chakrabartty, A., and Fraser, P. E. (1998) Phosphatidylinositol and inositol involvement in Alzheimer amyloid-β fibril growth and arrest. *J. Mol. Biol. 278*, 183–194.
23. Matsuzaki, K. (2007) Physicochemical interactions of amyloid β-peptide with lipid bilayers. *Biochim. Biophys. Acta 1768*, 1935–1942.
24. Kazlauskaite, J., Sanghera, N., Sylvester, I., Vénien-Bryan, C., and Pinheiro, T. J. T. (2003) Structural changes of the prion protein in lipid membranes leading to aggregation and fibrillization. *Biochemistry 42*, 3295–3304.
25. Lee, H.-J., Choi, C., and Lee, S.-J. (2002) Membrane-bound α-synuclein has a high aggregation propensity and the ability to seed the aggregation of the cytosolic form. *J. Biol. Chem. 277*, 671–678.
26. Necula, M., Chirita, C. N., and Kuret, J. (2003) Rapid anionic micelle-mediated α-synuclein fibrillization *in vitro*. *J. Biol. Chem. 278*, 46674–46680.
27. Lopes, D. H. J., Meister, A., Gohlke, A., Hauser, A., Blume, A., and Winter, R. (2007) Mechanism of islet amyloid polypeptide fibrillation at lipid interfaces studied by infrared reflection absorption spectroscopy. *Biophys. J. 93*, 3132–3141.
28. Knight, J. D., and Miranker, A. D. (2004) Phospholipid catalysis of diabetic amyloid assembly. *J. Mol. Biol. 341*, 1175–1187.
29. Knight, J. D., Hebda, J. A., and Miranker, A. D. (2006) Conserved and cooperative assembly of membrane-bound α-helical states of islet amyloid polypeptide. *Biochemistry 45*, 9496–9508.
30. Jayasinghe, S. A., and Langen, R. (2005) Lipid membranes modulate the structure of islet amyloid polypeptide. *Biochemistry 44*, 12113–12119.
31. Padrick, S. B., and Miranker, A. D. (2001) Islet amyloid polypeptide: Identification of long-range contacts and local order on the fibrillogenesis pathway. *J. Mol. Biol. 308*, 783–794.
32. Padrick, S. B., and Miranker, A. D. (2002) Islet amyloid: Phase partitioning and secondary nucleation are central to the mechanism of fibrillogenesis. *Biochemistry 41*, 4694–4703.
33. Jha, S., Sellin, D., Seidel, R., and Winter, R. (2009) Amyloidogenic propensities and conformational properties of proIAPP and IAPP in the presence of lipid bilayer membranes. *J. Mol. Biol. 389*, 907–920.
34. Williamson, J. A., Loria, J. P., and Miranker, A. D. (2009) Helix stabilization precedes aqueous and bilayer-catalyzed fiber formation in islet amyloid polypeptide. *J. Mol. Biol. 393*, 383–396.
35. Jaikaran, E. T. A. S., and Clark, A. (2001) Islet amyloid and type 2 diabetes: From molecular misfolding to islet pathophysiology. *Biochim. Biophys. Acta 1537*, 179–203.
36. Kajava, A. V., Aebi, U., and Steven, A. C. (2005) The parallel superpleated β-structure as a model for amyloid fibrils of human amylin. *J. Mol. Biol. 348*, 247–252.
37. Engel, M. F. M., Yigittop, H., Elgersma, R. C., Rijkers, D. T. S., Liskamp, R. M. J., de Kruijff, B., Höppener, J. W. M., and Killian, J. A. (2006) Islet amyloid polypeptide inserts into phospholipid monolayers as monomer. *J. Mol. Biol. 356*, 783–789.
38. Nanga, R. P. R., Brender, J. R., Xu, J., Veglia, G., and Ramamoorthy, A. (2008) Structures of rat and human islet amyloid polypeptide $IAPP_{1-19}$ in micelles by NMR spectroscopy. *Biochemistry 47*, 12689–12697.
39. Gorbenko, G. P., and Kinnunen, P. K. J. (2006) The role of lipid−protein interactions in amyloid-type protein fibril formation. *Chem. Phys. Lipids 141*, 72–82.
40. Rustenbeck, I., Matthies, A., and Lenzen, S. (1994) Lipid composition of glucose-stimulated pancreatic islets and insulin-secreting tumor cells. *Lipids 29*, 685–692.
41. Hull, R. L., Andrikopoulos, S., Verchere, C. B., Vidal, J., Wang, F., Cnop, M., Prigeon, R. L., and Kahn, S. E. (2003) Increased dietary fat promotes islet amyloid formation and β-cell secretory dysfunction in a transgenic mouse model of islet amyloid. *Diabetes 52*, 372–379.
42. Westermark, P. (1973) Fine structure of islets of Langerhans in insular amyloidosis. *Virchows Arch. A: Pathol. Anat. 359*, 1–18.
43. Clark, A., Lewis, C. E., Willis, A. C., Cooper, G. J. S., Morris, J. F., Reid, K. B. M., and Turner, R. C. (1987) Islet amyloid formed from diabetes-associated peptide may be pathogenic in type-2 diabetes. *Lancet 330*, 231–234.

44. Pozharski, E. V., McWilliams, L., and MacDonald, R. C. (2001) Relationship between turbidity of lipid vesicle suspensions and particle size. *Anal. Biochem. 291*, 158–162.
45. Levine, H., III (1999) Quantification of β-sheet amyloid fibril structures with thioflavin T. *Methods Enzymol. 309*, 274–284.
46. Ramstedt, B., and Slotte, J. P. (2002) Membrane properties of sphingomyelins. *FEBS Lett. 531*, 33–37.
47. Lewis, R. N. A. H., Zhang, Y.-P., and McElhaney, R. N. (2005) Calorimetric and spectroscopic studies of the phase behavior and organization of lipid bilayer model membranes composed of binary mixtures of dimyristoylphosphatidylcholine and dimyristoylphosphatidylglycerol. *Biochim. Biophys. Acta 1668*, 203–214.
48. Domanov, Y. A., and Kinnunen, P. K. J. (2008) Islet amyloid polypeptide forms rigid lipid-protein amyloid fibrils on supported phospholipid bilayers. *J. Mol. Biol. 376*, 42–54.
49. Yu, Z.-W., and Quinn, P. J. (1998) Solvation effects of dimethyl sulphoxide on the structure of phospholipid bilayers. *Biophys. Chem. 70*, 35–39.
50. Gordeliy, V. I., Kiselev, M. A., Lesieur, P., Pole, A. V., and Teixeira, J. (1998) Lipid membrane structure and interactions in dimethyl sulfoxide/water mixtures. *Biophys. J. 75*, 2343–2351.
51. Kayed, R., Head, E., Thompson, J. L., Mclntire, T. M., Milton, S. C., Cotman, C. W., and Glabe, C. G. (2003) Common structure of soluble amyloid oligomers implies common mechanism of pathogenesis. *Science 300*, 486–489.
52. Hall, D., and Edskes, H. (2009) A model of amyloids̀ role in disease based on fibril fracture. *Biophys. Chem. 145*, 17–28.
53. Apostolidou, M., Jayasinghe, S. A., and Langen, R. (2008) Structure of α-helical membrane-bound human islet amyloid polypeptide and its implications for membrane-mediated misfolding. *J. Biol. Chem. 283*, 17205–17210.
54. Engel, M. F. M., Khemtémourian, L., Kleijer, C. C., Meeldijk, H. J. D., Jacobs, J., Verkleij, A. J., de Kruijff, B., Killian, J. A., and Höppener, J. W. M. (2008) Membrane damage by human islet amyloid polypeptide through fibril growth at the membrane. *Proc. Natl. Acad. Sci. U.S.A. 105*, 6033–6038.
55. Brender, J. R., Lee, E. L., Cavitt, M. A., Gafni, A., Steel, D. G., and Ramamoorthy, A. (2008) Amyloid fiber formation and membrane disruption are separate processes localized in two distinct regions of IAPP, the type-2-diabetes-related peptide. *J. Am. Chem. Soc. 130*, 6424–6429.
56. Brender, J. R., Dürr, U. H. N., Heyl, D., Budarapu, M. B., and Ramamoorthy, A. (2007) Membrane fragmentation by an amyloidogenic fragment of human islet amyloid polypeptide detected by solid-state NMR spectroscopy of membrane nanotubes. *Biochim. Biophys. Acta 1768*, 2026–2029.